



Exploring the binding of peptidic West Nile virus NS2B–NS3 protease inhibitors by NMR



CongBao Kang^a, Shovanlal Gayen^a, Weiling Wang^a, Rene Severin^c, Angela Shuyi Chen^a, Huichang Annie Lim^a, Cheng San Brian Chia^a, Andreas Schüller^{b,1}, Danny Ngoc Phouc Doan^b, Anders Poulsen^a, Jeffrey Hill^a, Subhash G. Vasudevan^{b,*}, Thomas H. Keller^{a,*}

^a Experimental Therapeutics Center, 31 Biopolis Way, #03-01 Nanos, Singapore 138669, Singapore

^b Program in Emerging Infectious Diseases, Duke-NUS Graduate Medical School, Singapore 169857, Singapore

^c Institute of Chemical & Engineering Sciences, 11 Biopolis Way, #03-08 Helios, Singapore 138667, Singapore

ARTICLE INFO

Article history:

Received 10 October 2012

Revised 23 November 2012

Accepted 24 November 2012

Available online 2 December 2012

Keywords:

WNV protease
Peptide inhibitors
NMR study
Induced fit

ABSTRACT

West Nile virus (WNV) NS2B–NS3 protease is an important drug target since it is an essential protein for the replication of the virus. In order to determine the minimum pharmacophore for protease inhibition, a series of dipeptide aldehydes were synthesized. The 50% inhibitory concentration (IC₅₀) measurements revealed that a simple acetyl-KR-aldehyde was only threefold less active than 4-phenyl-phenylacetyl-KKR-aldehyde (**1**) (Stoermer et al., 2008) that was used as the reference compound. The ligand efficiency of 0.40 kcal/mol/HA (HA = heavy atom) for acetyl-KR-aldehyde is much improved compared to the reference compound **1** (0.23 kcal/mol/HA). The binding of the inhibitors was examined using ¹H-¹⁵N-HSQC experiments and differential chemical shifts were used to map the ligand binding sites. The biophysical studies show that the conformational mobility of WNV protease has a major impact on the design of novel inhibitors, since the protein conformation changes profoundly depending on the structure of the bound ligand.

© 2012 Elsevier B.V. All rights reserved.

1. Introduction

West Nile virus (WNV), a member of the flavivirus genus, is an arthropod-borne human pathogen first isolated from a febrile patient in the West Nile district of Uganda in 1937, and recognized in the mid 1950s to be the cause of severe meningitis and encephalitis in elderly patients in Israel. The virus was first introduced to the USA in 1999 and has seen an astounding proliferation to most of the states causing thousands of human infections (Gubler, 2007). Since neither a safe human vaccine nor a drug is available, the treatment of WNV infections is symptomatic, aimed at preventing clinical complications and reducing patient discomfort.

WNV is a small enveloped virus with a single-stranded, 11 kb RNA genome encoding a polyprotein processed by host and viral proteases (Robin et al., 2009). This polyprotein is cleaved into three structural proteins and seven nonstructural (NS) proteins including NS1, NS2A, NS2B, NS3, NS4A, NS4B and NS5 (Lindenbach et al.,

2007). The multifunctional NS3 protein that contains the protease activity needed for polyprotein processing is one of the most promising targets for drug discovery against flaviviral infections because of its important role in the replication process (Chambers et al., 1990). In addition the successful development of inhibitors against Hepatitis C virus protease (Perni et al., 2006), a member of the *flaviviridae* family, has further encouraged the search for protease inhibitors of WNV and dengue virus (DENV) serotypes.

The proteases of WNV and DENV have proven to be very challenging for drug discovery, due to the nature of the binding site that consists of shallow grooves on the protein surface. Although a number of potent peptide inhibitors have been described (Stoermer et al., 2008), all attempts to progress these chemical starting points towards high affinity peptidomimetics with acceptable pharmaceutical characteristics for oral delivery have not been successful. Similarly, the optimization of small molecular weight hits from high throughput screening (e.g. Su et al., 2009a,b; Ezgimen et al., 2012) has so far not provided any compounds with adequate potency for *in vivo* studies.

The active protease of WNV is formed by the interaction of NS3 and NS2B, both proteins contributing residues to the active site of the enzyme (Erbel et al., 2006; Chappell et al., 2008). In order to produce an active, stable protein for inhibition studies, 40 residues of NS2B have been tethered to the protease domain of NS3 by a flexible linker (WNV NS2B–NS3pro) (Nall et al., 2004). This artificial

* Corresponding authors. Address: Program in Emerging Infectious Diseases, Duke-NUS Graduate Medical School, 8 College Road, Singapore 169857, Singapore. Tel.: +65 6561 6718 (S.G. Vasudevan), tel.: +65 6407 0352 (T.H. Keller).

E-mail addresses: subhash.vasudevan@duke-nus.edu.sg (S.G. Vasudevan), thkeller@etc.a-star.edu.sg (T.H. Keller).

¹ Present address: Departamento de Genética Molecular y Microbiología, Facultad de Ciencias Biológicas, Pontificia Universidad Católica de Chile, Alameda 340, 8331150 Santiago, Chile.

WNV protease construct has proven to be a satisfactory mimic of the natural protein and has become the *de facto* standard for drug discovery (Nall et al., 2004). X-ray crystal structures have shown that this protein exhibits a very different protein fold in the apo-form than in complex with a peptide inhibitor (Benzoyl-Nle-KRR-aldehyde) (Erbel et al., 2006). NMR studies have confirmed the existence of an open and closed conformation and it has been shown that low molecular weight inhibitors shift the conformational exchange equilibrium towards the closed conformation (Su et al., 2009a,b). Only the closed conformation of NS2B–NS3pro is catalytically competent while in the open conformation the C-terminal region of NS2B detaches from NS3.

One of the reasons for the slow progress towards clinically useful WNV protease inhibitors is the lack of detailed structural information for a structure-guided drug discovery campaign. Although crystal structures are available with peptide aldehyde inhibitors (Erbel et al., 2006; Robin et al., 2009) and with aprotinin (Aleshin et al., 2007), attempts to use crystallography for the development and rationalization of structure activity relationships (SAR), as demonstrated during the discovery of HCV and HIV protease inhibitors (Tsantizos, 2008), have encountered difficulties because the WNV NS2B–NS3pro is not amenable to high throughput crystallization.

We have been searching for an alternative to X-ray crystallography in order to study the interaction of inhibitors with WNV protease and here we demonstrate the use of NMR spectroscopy to gain insight into the SAR of such compounds.

2. Methods and materials

2.1. Protein expression

The cDNA encoding the two-component WNV protease that contains 47 residues from NS2B, a G₄SG₄ linker and 184 residues from NS3 was cloned into the pET21d vector to generate pET21-WNV (Supplementary Fig. 1). pET21-WNV was chemically transformed into *Escherichia coli* BL21 (DE3) RILP codon plus competent cells and the cells were grown on a LB agar plate containing kanamycin (30 µg/ml). Two to three colonies were incubated in 30 ml of M9 medium with 30 µg/ml kanamycin. The overnight culture was further transferred into 1 L of M9 medium containing the antibiotic. When the OD₆₀₀ reached 0.6–0.8 induction was performed by adding β-D-1-thiogalactopyranoside (IPTG) to 1 mM final concentration, followed by incubation for 2 h at 25 °C. *E. coli* cells were harvested by centrifugation at 8000g for 10 min at 4 °C. The cell pellet was resuspended in a lysis buffer containing 20 mM sodium phosphate, pH 7.8, 500 mM NaCl, and 2 mM β-mercaptoethanol. Cells were lysed by sonication in an ice bath and the cell lysate was cleared by centrifugation at 40,000g for 20 min. The supernatant was passed through a gravity column containing Ni²⁺-NTA resin. Resin was washed with at least 10 column volumes of washing buffer containing 20 mM sodium phosphate, pH 7.8, 1 M NaCl, 10 mM imidazole and 2 mM β-mercaptoethanol to remove nonspecific binding proteins from the resin. Protein was eluted with an elution buffer containing 500 mM imidazole, pH 6.5, 500 mM NaCl and 2 mM β-mercaptoethanol. The purified protein was buffer exchanged to one containing 20 mM Tris–HCl, pH 7.8, 10 mM NaCl, 1 mM dithiothreitol (DTT) using a PD10 column. The protein was further purified using ion-exchange chromatography and then concentrated to 0.2–0.5 mM in an NMR buffer consisting of 20 mM HEPES, pH 7.3, 1 mM DTT and 10% D₂O.

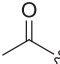
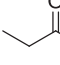

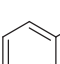
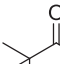
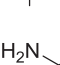
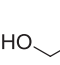
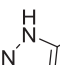
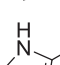
2.2. NMR experiments

For NMR studies, protein samples in an NMR buffer were transferred into 3 mm or 5 mm NMR tubes. All NMR spectra were ac-

quired at 298 K on a Bruker Avance II 700 MHz spectrometer equipped with a triple-resonance cryoprobe. The spectra were processed with Topspin 2.1 (Bruker) and NMRPipe (Delaglio et al., 1995), and visualized with NMRView (Johnson, 2004) or Sparky (<http://www.cgl.ucsf.edu/home/sparky/>). For backbone assignment of WNV, protease inhibitor **1** was added to a final concentration of 2 mM, by adding a 30 mM stock solution prepared in NMR buffer or d₆-DMSO to 0.8 mM triple-labeled WNV protease. The backbone ¹HN, ¹⁵N and ¹³Cα resonances were assigned using two dimensional (2D) and Transverse Relaxation Optimized Spectroscopy (TROSY) (Pervushin et al., 1997)-based three dimensional (3D) experiments including ¹H-¹⁵N-HSQC (heteronuclear single quantum coherence), 3D-HNCACB, CBCA(CO)NH, and HNCA experiments. All the pulse programs were from the Bruker standard library. Protein secondary structure was analyzed using Talos+ (Shen et al., 2009) and chemical shift index analysis was performed by comparing the deviation of the Ca values from the random coil values (Wishart et al., 1992).

To obtain distance restraints between WNV protease and inhibitor **1**, 3D ¹⁵N(F1)-edited/¹⁵N(F3)-filtered NOESY was acquired. A 0.5 mM ¹⁵N/¹³C/²H-labeled WNV protease solution in NMR buffer was mixed with a 2 mM solution of inhibitor **1** in NMR buffer and data was acquired with a mixing time of 100 ms (Iwahara et al., 2001). The unambiguous NOEs between protease and inhibitor **1** were used to analyze the models from a docking study. To compare the chemical shift difference from different inhibitors, ¹H-¹⁵N-HSQC spectra of 0.2 mM WNV protease in the presence and absence of 1 mM inhibitors were collected and superimposed. All the inhibitors were dissolved in the NMR buffer, except for some inhibitors with lower solubility were dissolved in d₆-DMSO.

Table 1
Inhibition of WNV protease by X-KR-aldehyde inhibitors.

Inhibitor	X	IC ₅₀ (µM) ^a	Ligand efficiency (LE) ^{b,c}
2		0.17 ± 0.04	0.40
3		0.34 ± 0.10	0.37
4		0.43 ± 0.09	0.35
5		1.84 ± 0.18	0.28
6		1.53 ± 0.08	0.31
7		5.84 ± 0.76	0.30
8		0.25 ± 0.02	0.38
9		0.22 ± 0.02	0.34
10		0.12 ± 0.01	0.35

^a Average of three independent determinations.

^b Calculated as described in Hopkins et al., 2004.

^c kcal/mol/HA (HA = heavy atom).

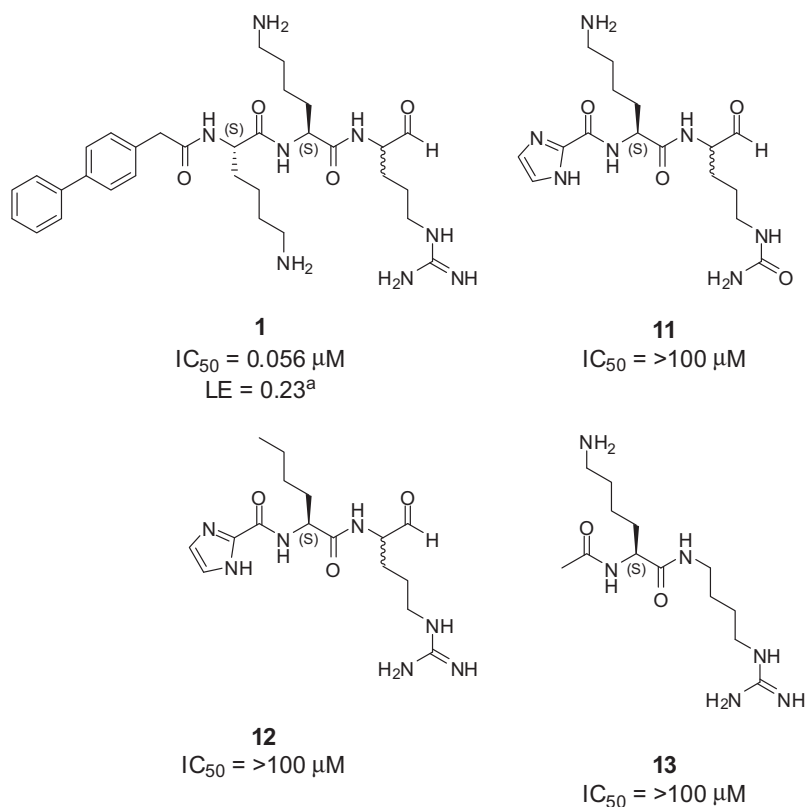


Fig. 1. Structures of tripeptide **1** and dipeptides **11**, **12** and **13** with the respective IC_{50} 's. ^aLigand efficiency (Hopkins et al., 2004) is given in kcal/mol/HA (HA = heavy atom).

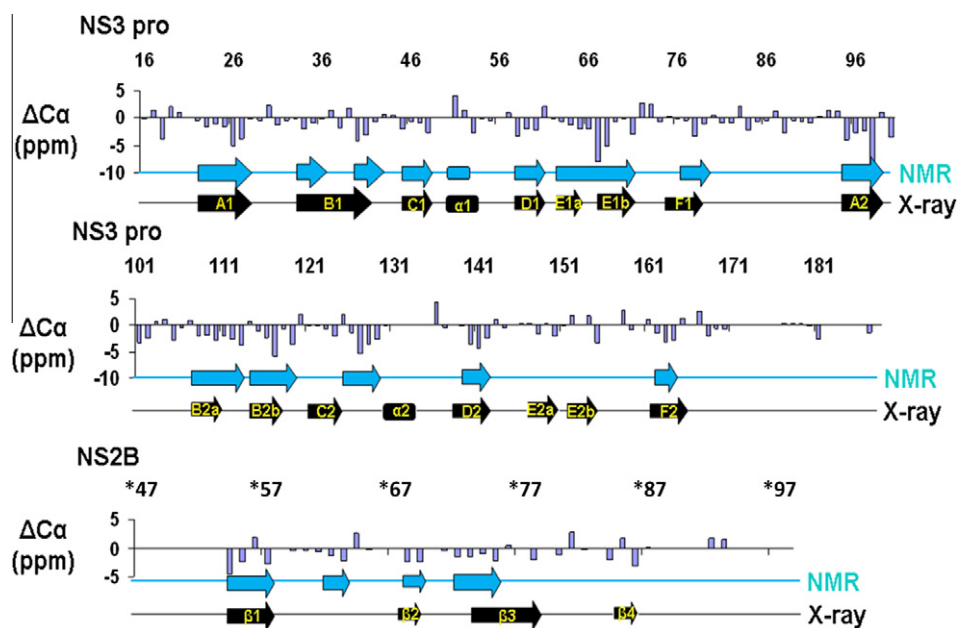


Fig. 2. Secondary structure analysis of WNV protease. Chemical shift index analysis of the protease/inhibitor complex was conducted based on the backbone assignment (inhibitor = compound **1**). Positive $\Delta C\alpha$ indicate the existence of alpha helical structures, while negative values indicate the existence of a beta sheet. Secondary structure assignment from the NMR experiments is shown in light blue, and in black the secondary structure from the X-ray crystal structure (PDB: 3E90) (Robin et al., 2009) is included. The secondary structure nomenclature shown in yellow was adapted from the literature (Aleshin et al., 2007). (For interpretation of color in Fig. 2, the reader is referred to the web version of this article.)

2.3. WNV protease assay

The WNV protease enzyme activity assay was performed in a final volume of 30 μl in a 384 well black microtiter plate. The com-

pounds dissolved in 100% DMSO were tested at different concentrations. 1 μl compound and 19 μl of 10 nM of enzyme in 50 mM Tris-HCl, pH 8.5, 20% glycerol and 1 mM CHAPS were added to 384 well plate and pre-incubated at 30 °C for 15 min.

The reaction was initiated by the addition of 10 μ l of Benzoyl-Nle-KRR-AMC to a final concentration of 20 μ M to each well and the plate was incubated at 30 °C for another 30 min. Release of AMC, which indicates the proteolytic cleavage was monitored by measuring the fluorescence at 380 nm (excitation) and 450 nm (emission) wavelength in a Tecan Infinite M200 Microplate Reader. The assay was performed in triplicate. Benzoyl-Nle-KRR-aldehyde was included as a positive control. A control reaction was performed with all the components except the enzyme. Percentage inhibition was calculated using a negative control (0% activity) and enzyme reaction (100% activity).

2.4. Molecular modeling

The WNV protease X-ray structure PDB entry 3E90 (Robin et al., 2009) was downloaded from the Protein Data Bank [www.pdb.org] and prepared with the protein preparation wizard in Maestro 9.3 (Schrödinger et al., 2012) using standard settings. This included the addition of hydrogen atoms, bond assignments, removal of water molecules further than 7 Å from the ligand, protonation state assignment, optimization of the hydrogen bond network and restrained minimization using the OPLS2005 force field (Kaminski et al., 2001). The co-crystallized, covalently bound inhibitor was replaced with the dipeptide inhibitors by using the conformation of the co-crystallized ligand as a template. The covalently bound inhibitor-protein complex was finally minimized using MacroModel 9.9 (Schrödinger et al., 2012). All residues more than 7 Å from the ligand were constrained before the complex was subjected to 500 steps of Polak-Ribiere-Conjugate-Gradient (Polak and Ribiere, 1969) minimization using the OPLS2005 force field and GB/SA continuum solvation model (Hasel et al., 1988).

2.5. Peptide aldehyde synthesis

Dipeptide aldehydes were synthesized, purified and characterized according to procedures reported in a recent paper (Schüller et al., 2011).

3. Results and discussion

As a first step towards peptidomimetic inhibitors, we have attempted to reduce the size of the high affinity peptides reported by Stoermer and co-workers (e.g. **1**) (Stoermer et al., 2008) in order to better understand the minimum requirements for tight binding. The identification of a chemical starting point with high ligand efficiency (small molecular weight and high potency; Hopkins et al., 2004) is especially important in this case, since the aldehyde and one of the highly basic groups need to be replaced to obtain a stable inhibitor with oral activity. Table 1 summarizes the inhibition of WNV protease by nine novel dipeptides with the general structure X-KR-aldehyde, where X denotes different cap groups. When these results are compared with the reference peptide 4-phenyl-phenylacetyl-KKR-aldehyde (**1**) (Stoermer et al., 2008) (Fig. 1), which in our hands had an IC_{50} of 56 nM, it is clear that the P3 lysine and the hydrophobic cap group in **1** contribute very little to the observed inhibition constant. The simple dipeptide **2** is only threefold less active but has a much improved ligand efficiency of 0.40 kcal/mol/HA (HA = heavy atom) as compared to the 0.23 kcal/mol/HA for **1**. Overall small capping groups are clearly preferred while the bulky pivaloyl but also the phenyl cap leads to a more than 10-fold reduction in IC_{50} .

While the inhibitory activity of peptides with different caps can be rationalized (Table 1), the SAR resulting from changes in other parts of the inhibitors is more difficult to understand. For example compounds **11** and **12** were synthesized to study the molecular

recognition in the S1 and S2 pockets, and compound **13** (Fig. 1) was designed to investigate the contribution of the aldehyde war-head toward the potency of the dipeptide (Lim et al., 2011). All of these changes lead to a total loss of activity in the enzymatic assay. Such modifications also lead to a reduction in activity for tripeptide aldehydes (Knox et al., 2006; Stoermer et al., 2008) however our dipeptides seem to be more sensitive toward changes in the S1 or S2 pocket.

Since SAR is an important tool for the optimization of compounds, the binary nature of changes (active–inactive) in the P1 or P2 site is quite discouraging. It is clear that a useful replacement for arginine and lysine can only be found if a tool can be identified that allows the medicinal chemists to distinguish between different isosteric replacements. Clearly the enzymatic assay alone is not sensitive enough for this task. When all attempts to obtain X-ray crystal structures with the dipeptides were unsuccessful, we turned our attention to NMR based methods, which are known to be especially useful for the study of weak binding ligands (Shuker et al., 1996). In addition, NMR spectroscopy can be useful for tracking conformational changes of proteins resulting from ligand binding (Pellecchia et al., 2002).

As a first step we investigated the 1H - ^{15}N -HSQC (heteronuclear single quantum coherence) spectra of WNV NS2B–NS3pro in the presence or absence of the peptide inhibitor **1** (Supplementary

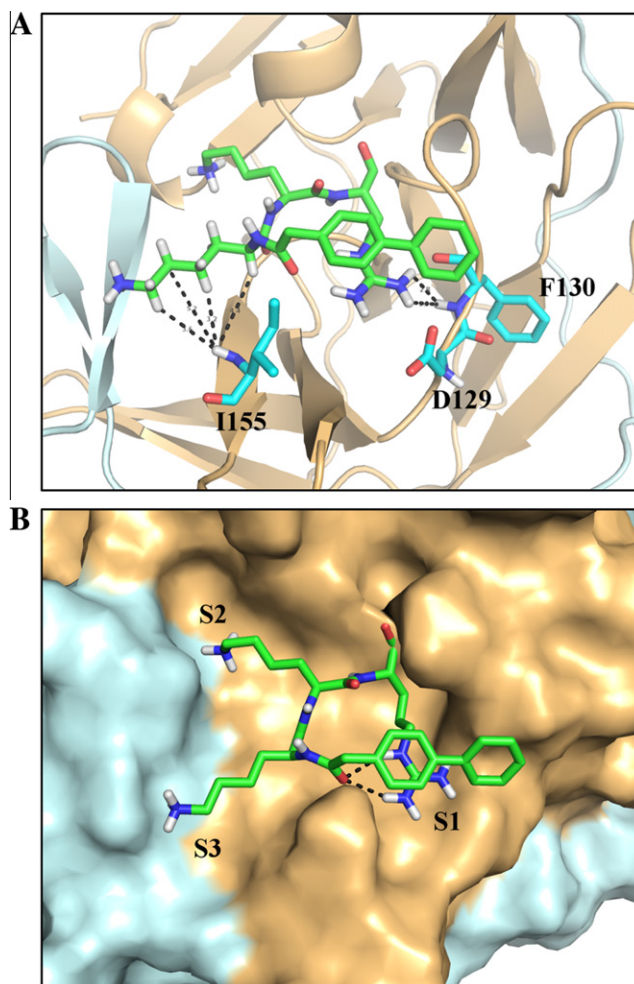


Fig. 3. Inhibitor **1** (light green) docked into the WNV protease (NS3 in light brown; NS2B in light blue). (A) Ribbon diagram showing the amino acids involved in the NOE signals in turquoise and filtered NOE as dashed black lines; (B) Same view of the active site as A but as solvent accessible surface; dashed black lines illustrate intramolecular hydrogen bonding.

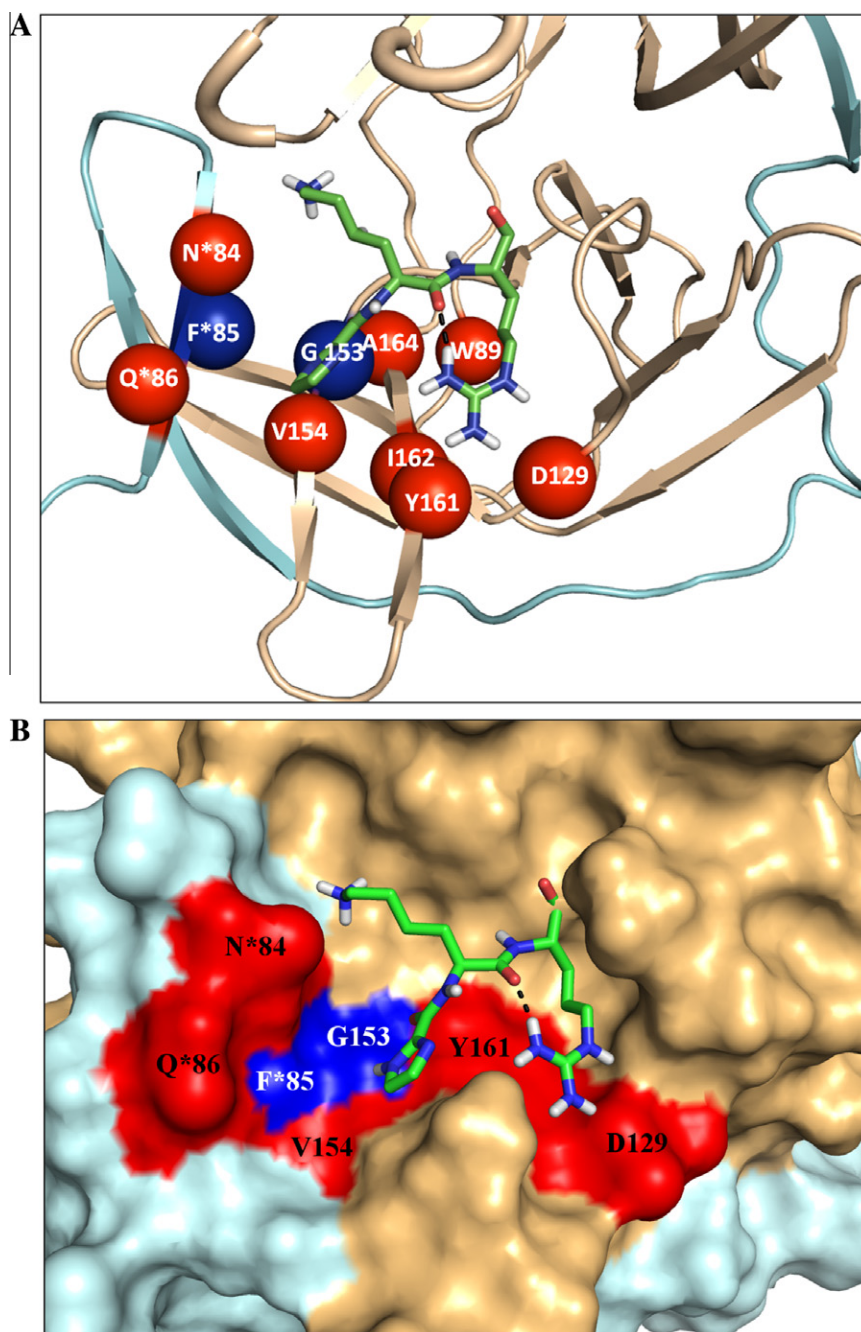


Fig. 4. (A) Ribbon diagram of WNV protease with docked dipeptide **10** (NS3 = light brown; NS2B = light blue); Red spheres depict amino acid residues (aa) which show $\alpha > 0.1$ ppm shift when the HSQC spectra of **1** and **10** are compared; blue spheres denote aa which are visible in the spectrum of **1**, but absent in **10**. (B) Same representation as in A, but with a solvent accessible surface showing the conformational flexibility in the active site; red surface depicts aa's that show a shift of >0.1 ppm and blue areas represent aa that disappear from the HSQC spectrum of **10**. The comparison between A and B allows one to distinguish between internal and aa's on the enzyme surface.

Fig. 2). The backbone resonances in the presence of **1** were assigned using conventional NMR experiments (Fig. 2, Supplementary Fig. 3). We obtained approximately 80% assignment for the backbone resonances of WNV protease and the assignment was deposited in the Biological Magnetic Resonance Bank (BMRB) with accession number 18730. Secondary structure analysis from chemical shift index (CSI) of the $C\alpha$ backbone atoms indicated that the NMR structure of WNV protease is similar to the crystal structure (Robin et al., 2009) (Fig. 2). In order to obtain the tertiary structure of the protein in complex with **1**, we performed a docking study based on restraints between inhibitor **1** and the protease from fil-

tered NOE experiments (Fig. 3, Supplementary Fig. 4). In order to differentiate the numbering of the sequences of NS2B and NS3, a prefix of * was added to the sequence numbers for NS2B (see also Supplementary Fig. 1).

With the NMR structural information in hand, we decided to use differential chemical shifts (Pellecchia et al., 2002) to map the ligand binding sites of selected dipeptides (Table 1). As previously reported by Otting and co-workers (Su et al., 2009a) the NMR signals of WNV NS2B–NS3pro can be broadened beyond detection by conformational dynamics in the absence an inhibitor. The spectra improve dramatically through the formation of com-

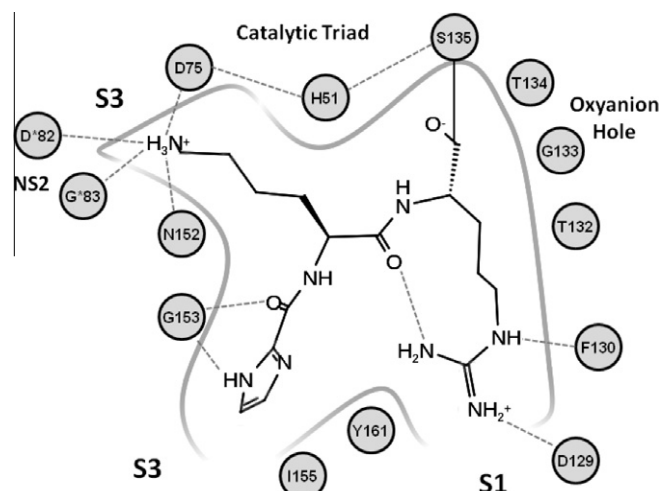


Fig. 5. Interaction map of inhibitor **10** with WNV protease. Hydrogen bonds are depicted as dashed lines. The illustration represents the docked dipeptide **10** in the active site of WNV protease, and is in agreement with all of the NMR findings.

plexes with inhibitors, depending on the ability of compounds to shift the conformational exchange equilibria towards a single conformer. Through the observation of chemical shifts or line broadening (disappearing peaks), we can study the conformational changes of the protein as a result of its interaction with a peptide aldehyde inhibitor.

When the result of the binding studies for the most potent dipeptide inhibitor **10** was compared with the results of our NMR study with **1**, chemical shift perturbations were observed in residues Q*86, N*84, T*57, A164, I162, Y161, V154, D129, W89 while the signal of F*85 and G153 had disappeared (Fig. 4, Supplementary Figs. 5 and 6). Since the major difference between **1** and **10** is the missing lysine in the S3 pocket, it is not surprising that the major chemical shift perturbations are seen in that region (Fig. 4). The changes observed in the S1 pocket (D129, Y161) were somewhat unexpected, but can be explained by molecular modeling. As can be seen in the interaction map (Fig. 5), dipeptide **10** forms an internal hydrogen bond between arginine and the carbonyl of the P2 lysine, which leads to a reorientation of the P1 amino acid relative to **1** (compare Figs. 3 and 4B), causing the observed perturbation in the chemical shift in D129 and Y161.

The exquisite sensitivity of the NMR can be seen when **2** and **10** are compared (Supplementary Fig. 7). These two dipeptides have slightly different caps (acetyl vs. 2-imidazolyl) and very similar IC_{50} values (0.17 μ M vs. 0.12 μ M), however chemical shift perturbations > 0.1 ppm are observed for I162, Y161, M156 and N152 (Supplementary Fig. 7). Since all of these amino acids are located in the same E2B–F2 loop (see Fig. 7 for naming convention), the data suggests that the change in cap residues leads to a conformational change between N152 and I162 (Fig. 6A, Supplementary Fig. 7). This can be easily rationalized since molecular modeling suggests that the 2-imidazolyl cap (compound **10**) forms a hydrogen bond with G153 (Fig. 5), which is absent in **2**.

With a good understanding of the binding of the potent inhibitors **2** and **10**, we turned our attention to the derivatives that were shown to be inactive in the enzymatic assay. In accordance with the assay result, dipeptide **11** did not show any interaction with the WNV protease in the NMR experiment (Supplementary Fig. 8). This finding is in agreement with the literature (Knox et al., 2006; Stoermer et al., 2008), and it again demonstrates the importance of the cationic functional group in the S1 pocket. The single atom change (N in **2**; O in **11**) abrogates any binding of the peptide to the protease, suggesting that electrostatic interactions play a crucial role in protease binding.

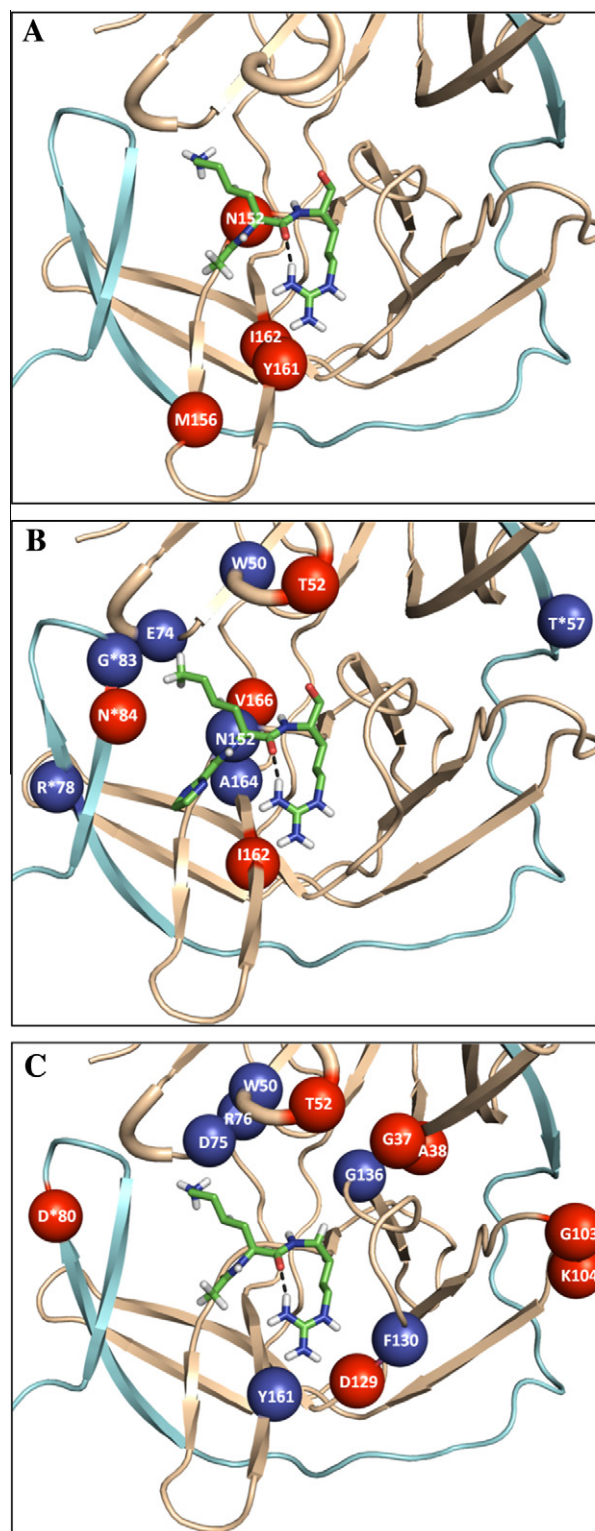


Fig. 6. Peptides (light green) docked into the WNV protease depicted as a ribbon diagram (NS3 in light brown; NS2B in light blue). (A) Differential chemical shifts when comparing the HSQC spectra of **10** and **2**; Red spheres depict amino acids (aa) which show $a > 0.1$ ppm shift when the HSQC spectra of **10** and **2** are compared. (B) Differential chemical shifts when comparing the HSQC spectra of **10** and **12**; Red spheres depict amino acids which show $a > 0.1$ ppm shift when the HSQC spectra of **10** and **12** are compared; blue spheres denote aa's which are visible in the spectrum of **10**, but absent in **12**. (C) Differential chemical shifts when comparing the HSQC spectra of **10** and **13**; Red spheres depict aa which show $a > 0.1$ ppm shift when the HSQC spectra of **10** and **13** are compared; blue spheres denote aa's which are visible in the spectrum of **10**, but absent in **13**.

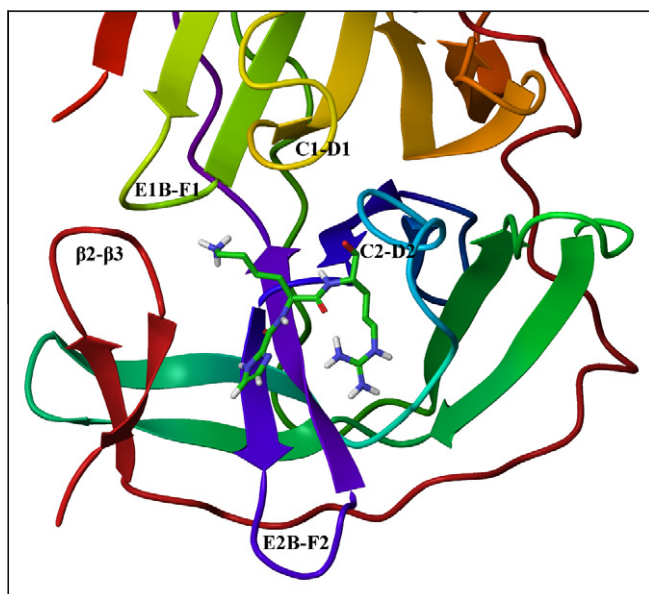


Fig. 7. The structure of WNV protease in complex with inhibitor **10**. Secondary structure elements are named according to Aleshin et al., 2007.

In contrast to **11**, dipeptides **12** and **13** show clear binding in the HSQC-experiments even though they are not able to inhibit the WNV protease in the assay (Supplementary Figs. 9 and 10). In order to better understand the molecular recognition of **12**, we compared its NMR spectra with the closely related analogue **10**. Even though the only difference between these two molecules is the absence of the basic NH_2 group in the S2 pocket (Table 1; Fig. 5) there is a 1000-fold difference in their IC_{50} values. The differential shifts in T*57, R*78, G*83, N*84, W50, T52, E74, N152, I162, A164, and V166 from the NMR experiments (Fig. 6B) clearly show that the removal of the amine causes a major conformational change, not only in the NS2B loop (β 2- β 3) between R*78 and N*84, which is in direct contact with **10** in the S2-pocket (Fig. 5), but also in parts of the NS3 protein that are adjacent to the binding site (Fig. 6B). For example N152 of NS3 are within hydrogen bonding distance of the P2 residue in **10** (P2-lysine) but not so in **12** (P2-norleucine), which explains the absence of the N152 NMR signal in the spectrum of **12**.

The conformational mobility of WNV NS2B–NS3pro is further illustrated by dipeptide **13**, which differs from the potent inhibitor **10** by the absence of the aldehyde, which is thought to be a major contributor to inhibitor binding by forming a transition state analogue with S135 of the catalytic triad (Leung et al., 2000). The absence of this group in **13** leads to a total loss of activity in the enzymatic assay ($\text{IC}_{50} > 100 \mu\text{M}$ vs. $0.17 \mu\text{M}$ for compound **10**). The chemical shift perturbations (comparing **10** and **13**; involving amino acids D*80, G37, A38, W50, T52, D75, R76, G103, K104, D129, F130, G136 and Y161) again suggest that the loss of activity is accompanied by significant conformational changes in the peptide binding site of the NS3 protein (Fig. 6C, Supplementary Table 1). This conformational mobility affects the S1 pocket (absent NMR signals of F130 and Y161, and chemical shift perturbation of D129), partly the S2 pocket (absent signals of D75, differential chemical shift of D*80, β 2- β 3 loop) and the region of the catalytic triad. The signal of G136, the amino acid just next to S135 of the catalytic triad, disappears in the spectra of **13**. The three-dimensional structure of NS3pro adopts a chymotrypsin-like fold with two β -barrels and G136 sits at the interface of the C-terminal β -barrel facing two amino acids with differential chemical shifts (G37 and A38, β -sheet B1) on the N-terminal β -barrel within van der Waals contact distance. Differential chemical shifts of W50

and T52 are explained by their proximity to H51, the second amino acid of the catalytic triad. The signal of D75, the third amino acid of the catalytic triad, and R76, next in the sequence, are absent in the spectra of **13**, as well.

4. Conclusion

Despite the available structural information, the optimization of both peptidic and small-molecule inhibitors of WNV protease has been challenging because the observed structure activity relationships are difficult to rationalize. In this study we have used NMR techniques to gain insights into the changes in protein conformation in response to inhibitor binding. These biophysical studies suggest that inhibitors play a major role in maintaining the integrity of the active site of the enzyme. Furthermore, changes to the inhibitor structures can promote conformational rearrangement of the protein loops defining the enzyme active site, abrogating inhibitory activities (Fig. 7).

Our results show that P3 residues are not necessary for potent inhibition of the enzyme, even though chemical shift perturbations indicative of conformational change (Fig. 4) are observed in the E2B-F2 loop of NS3 (Fig. 7; purple) and the β 2- β 3 loop of NS2B (Fig. 7; red) when the P3 residue is removed. The latter finding is not surprising since the E2B-F2 loop is known to be an area of general structural mobility of flaviviral NS2B–NS3 proteases (Erbel et al., 2006; Robin et al., 2009; Aleshin et al., 2007). The most potent dipeptide inhibitors (e.g. **2** and **10**) seem to retain the key recognition elements for effective inhibition of the protease. However, further manipulation of the remaining basic amino acids is not tolerated, as illustrated by compound **11**, where the mutation of a single atom (N–O) leads to the loss of a salt bridge between **11** and the C2-D2 loop, resulting in a compound that does not show any affinity for the protein. The sensitivity of the WNV protease to small changes in the active site is also demonstrated by compound **12**, where the amine responsible for hydrogen bonding in the S2 pocket has been removed. The absence of this amine has a major impact on the conformation of the substrate binding site with reorganization of the β 2- β 3 and the E1B-F1 loop which form part of the S2 pocket, but also of the C1-D1 loop which points to a perturbation of the catalytic triad. Low-affinity dipeptide **13** with an absent aldehyde warhead further underlines this tendency. Comparing its NMR spectra with a high-affinity dipeptide indicates significant conformational mobility in the loops forming the S1 and S2 pockets, and in the formation of the catalytic triad. Furthermore, conformational plasticity here also spreads to areas not directly in contact with the substrate binding site (e.g. β -sheet B1).

Overall these findings are in agreement with the induced-fit mechanism of substrate/inhibitor binding as proposed by Strongin and coworkers (Aleshin et al., 2007) for the WNV protease. The conformational mobility of the protein has a major impact on inhibitor design, since compounds that do not interact with the relevant loops (Fig. 7) cannot compete in a meaningful way with the substrate peptides. Until the conformational behavior of the protein is better understood, the development of potent non-peptidic inhibitors either by structure-based design or traditional SAR-driven optimization will be difficult. Since the active site is stabilized by the substrates, it may be a better strategy to aim for allosteric inhibitors, which lock the protease in a conformation(s) that cannot be used for the processing of the viral polyprotein.

Appendix A. Supplementary data

Supplementary data associated with this article can be found, in the online version, at <http://dx.doi.org/10.1016/j.antiviral.2012.11.008>.

References

- Aleshin, A.E., Shiryayev, S.A., Strongin, A.Y., Liddington, R.C., 2007. Structural evidence for regulation and specificity of flaviviral proteases and evolution of the Flaviviridae fold. *Protein Sci.* 16, 795–806.
- Chambers, T.J., Weir, R.C., Grakoui, A., McCourt, D.W., Bazan, J.F., Fletterick, R.J., Rice, C.M., 1990. Evidence that the N-terminal domain of nonstructural protein NS3 from yellow fever virus is a serine protease responsible for site-specific cleavages in the viral polyprotein. *Proc. Natl. Acad. Sci. USA* 87, 8898–8902.
- Chappell, K.J., Stoermer, M.J., Fairlie, D.P., Young, P.R., 2008. Mutagenesis of the West Nile virus NS2B cofactor domain reveals two regions essential for protease activity. *J. Gen. Virol.* 89, 1010–1014.
- Delaglio, F., Grzesiek, S., Vuister, G.W., Zhu, G., Pfeifer, J., Bax, A., 1995. NMRPipe: a multidimensional spectral processing system based on UNIX pipes. *J. Biomol. NMR* 6, 277–293.
- Erbel, P., Schiering, N., D'Arcy, A., Renatus, M., Kroemer, M., Lim, S.P., Yin, Z., Keller, T.H., Vasudevan, S.G., Hommel, U., 2006. Structural basis for the activation of flaviviral NS3 proteases from dengue and West Nile virus. *Nat. Struct. Mol. Biol.* 13, 372–373.
- Ezgin, M., Lai, H., Mueller, N.H., Lee, K., Cuny, G., Ostrov, D.A., Padmanabhan, R., 2012. Characterization of the 8-hydroxyquinoline scaffold for inhibitors of West Nile Virus serine protease. *Antivir. Res.* 94, 18–24.
- Gubler, D.J., 2007. The continuing spread of West Nile Virus in the Western Hemisphere. *Clin. Infect. Dis.* 45, 1039–1046.
- Hasel, W., Hendrickson, T.F., Still, W.C., 1988. A rapid approximation to the solvent accessible surface areas of atoms. *Tetrahedron Comput. Method.* 1, 103–116.
- Hopkins, A.L., Groom, C.R., Alex, A., 2004. Ligand efficiency: a useful metric for lead selection. *Drug Discov. Today* 9, 430–431.
- Iwahara, J., Wojciak, J.M., Clubb, R.T., 2001. Improved NMR spectra of a protein-DNA complex through rational mutagenesis and the application of a sensitivity optimized isotope-filtered NOESY experiment. *J. Biomol. NMR* 19, 231–241.
- Johnson, B.A., 2004. Using NMRView to visualize and analyze the NMR spectra of macromolecules. *Methods Mol. Biol.* 278, 313–352.
- Kaminski, G.A., Friesner, R.A., Tirado-Rives, J., Jorgensen, W.L., 2001. Evaluation and reparametrization of the OPLS-AA force field for protein via comparison with accurate quantum chemical calculations on peptides. *J. Phys. Chem. B* 105, 6474–6487.
- Knox, J.E., Ma, N.L., Yin, Z., Patel, S.J., Wang, W.L., Chan, W.L., Rao, K.R.R., Wang, G., Ngew, X., Patel, V., Beer, D., Lim, S.P., Vasudevan, S.G., Keller, T.H., 2006. Peptide inhibitors of West Nile NS3 protease: SAR study of tetrapeptide aldehyde inhibitors. *J. Med. Chem.* 49, 6585–6590.
- Leung, D., Abbenante, G., Fairlie, D.P., 2000. Protease inhibitors: current status and future prospects. *J. Med. Chem.* 43, 305–341.
- Lim, H.A., Joy, J., Hill, J., Chia, C.S.B., 2011. Novel agmatine and agmatine-like peptidomimetic inhibitors of the West Nile virus NS2B/NS3 serine protease. *Eur. J. Med. Chem.* 46, 3130–3134.
- Lindenbach, B.D., Thiel, H.J., Rice, C.M., 2007. Flaviviridae: the viruses and their replication. In: Knipe, D.M., Howley, P.M. (Eds.), *Fields Virology*, 5th Edition. Lippincott-Raven Publishers, Philadelphia, pp. 1101–1152.
- Nall, T.A., Chappell, K.J., Stoermer, M.J., Fang, N.X., Tyndall, J.D.A., Young, P.R., Fairlie, D.P., 2004. Enzymatic characterization and homology model of a catalytically active recombinant West Nile virus NS3 protease. *J. Biol. Chem.* 279, 48535–48542.
- Pellecchia, M., Sem, D.S., Wüthrich, K., 2002. NMR in drug discovery. *Nat. Rev. Drug Discov.* 1, 211–218.
- Perni, R.B., Almquist, S.J., Byrn, R.A., Chandorkar, G., Chaturvedi, P.R., Courtney, L.F., Decker, C.J., Dinehart, K., Gates, C.A., Harbeson, S.L., Heiser, A., Kalkeri, G., Kolaczowski, E., Lin, K., Luong, Y.P., Rao, B.G., Taylor, W.P., Thomson, J.A., Tung, R.D., Wei, Y., Kwong, A.D., Lin, C., 2006. Preclinical profile of VX-950, a potent, selective, and orally bioavailable inhibitor of hepatitis C virus NS3-4A serine protease. *Antimicrob. Agents Chemother.* 50, 899–909.
- Pervushin, K., Riek, R., Wider, G., Wüthrich, K., 1997. Attenuated T2 relaxation by mutual cancellation of dipole-dipole coupling and chemical shift anisotropy indicates an avenue to NMR structures of very large biological macromolecules in solution. *Proc. Natl. Acad. Sci. USA* 94, 12366–12371.
- Polak, E., Ribiere, G., 1969. Note sur la Convergence de Méthodes de Directions Conjuguées. *Rev. Fr. Inform. Rech. O Série Rouge* 16, 35–43.
- Robin, G., Chappell, K., Stoermer, M.J., Hu, S.H., Young, P.R., Fairlie, D.P., Martin, J.L., 2009. Structure of West Nile Virus NS3 protease: ligand stabilization of the catalytic conformation. *J. Mol. Biol.* 385, 1568–1577.
- Schüller, A., Yin, Z., Chia, C.S.B., Doan, D.N.P., Kim, H.-K., Shang, L., Loh, T.P., Hill, J., Vasudevan, S.G., 2011. Tripeptide inhibitors of dengue and West Nile virus NS2B–NS3 protease. *Antiviral Res.* 92, 96–101.
- Schrödinger, LLC., 2012. New York, NY, USA, <www.schrodinger.com>.
- Shen, Y., Delaglio, F., Cornilescu, G., Bax, A., 2009. TALOS+: a hybrid method for predicting protein backbone torsion angles from NMR chemical shifts. *J. Biomol. NMR* 44, 213–223.
- Shuker, S.B., Hajduk, P.J., Meadows, R.P., Fesik, S.W., 1996. Discovering high-affinity ligands for proteins: SAR by NMR. *Science* 274, 1531–1534.
- Stoermer, M.J., Chappell, K.J., Liebscher, S., Jensen, C.M., Gan, C.H., Gupta, P.K., Xu, W.J., Young, P.R., Fairlie, D.P., 2008. Potent cationic inhibitors of West Nile Virus NS2B/NS3 protease with serum stability, cell permeability and antiviral activity. *J. Med. Chem.* 51, 5714–5721.
- Su, X.C., Ozawa, K., Yagi, H., Lim, S.P., Wen, D., Ekonomiuk, D., Huang, D., Keller, T.H., Sonntag, S., Caffisch, A., Vasudevan, S.G., Otting, G., 2009a. NMR study of complexes between low molecular mass inhibitors and the West Nile Virus NS2B–NS3 protease. *FEBS J.* 276, 4244–4255.
- Su, X.C., Ozawa, K., Qi, R., Vasudevan, S.G., Lim, S.P., Otting, G., 2009b. NMR analysis of the dynamic exchange of the NS2B cofactor between open and closed conformations of the West Nile Virus NS2B–NS3 protease. *PLoS Negl. Trop. Dis.* 3, e561.
- Tsantrizos, Y.S., 2008. Peptidomimetic therapeutic agents targeting the protease enzyme of the human immunodeficiency virus and hepatitis C virus. *Acc. Chem. Res.* 41, 1252–1263.
- Wishart, D.S., Sykes, B.D., Richards, F.M., 1992. The chemical shift index: a fast and simple method for the assignment of protein secondary structure through NMR spectroscopy. *Biochemistry* 31, 1647–1651.